Pressure tuning of the charge density wave and superconductivity in 2*H*-TaS_2

Xiao-Miao Zhao,[1,2,3] Kai Zhang,[2] Zi-Yu Cao,[2] Zhi-Wei Zhao,[1] Viktor V. Struzhkin,[3] Alexander F. Goncharov,[3] Hai-Kuo Wang,[1] Alexander G. Gavriliuk,[4,5] Ho-Kwang Mao,[2,3] and Xiao-Jia Chen[2,6,3,*]

[1]*College of Materials Science and Engineering, Henan University of Technology, Zhengzhou 450001, China*
[2]*Center for High Pressure Science and Technology Advanced Research, Shanghai 201203, China*
[3]*Geophysical Laboratory, Carnegie Institution of Washington, Washington DC 20015, USA*
[4]*Institute for Nuclear Research, Russian Academy of Sciences, Moscow, Troitsk 108840, Russia*
[5]*FSRC Crystallography and Photonics of Russian Academy of Sciences, Moscow 119333, Russia*
[6]*Key Laboratory of Materials Physics, Institute of Solid State Physics, Chinese Academy of Science, Hefei 230031, China*

(Received 17 September 2019; revised manuscript received 14 January 2020; accepted 25 March 2020; published 13 April 2020)

Both the vibrational and electrical transport properties of 2*H*-TaS_2 have been investigated at high pressures and low temperatures. The collapse of the charge-density-wave order at pressures above 7.3 GPa has been verified by Raman scattering, resistivity, and Hall coefficient measurements. For pressures above the critical pressure of 7.3 GPa, the superconducting transition temperature continues to increase and reaches its maximum value at 11.5 GPa, suggesting that it is not a simple competition between the charge-density-wave order and superconductivity. Through the standard resistivity fit in the normal state, the decline of the superconducting transition temperature with increasing pressure up to 47.0 GPa is due to the decrease of interaction strength and the increase of the impurity scattering. These results are very important in understanding the superconducting mechanism of transition-metal dichalcogenides.

DOI: 10.1103/PhysRevB.101.134506

The interplay between the charge-density-wave (CDW) order and superconductivity has received enormous attention for several decades in condensed-matter physics. Transition-metal dichalcogenides (TMDs), especially the 2*H* polytype of TMDs with complex electronic behaviors, present the coexistence of the CDW and superconductivity at low temperature, providing an ideal platform to investigate the interplay of these quantum phases [1–4]. CDWs are periodic modulations of the electronic charge density at the atomic sites, accompanied by a distortion of the crystal lattice. For the CDW-bearing TMDs, both the origin of the CDW order and the interplay between the CDW and superconductivity play essential roles in understanding the mechanism of superconductivity. Many theoretical models were proposed to explain the formation of the CDW, such as strong electron-phonon interactions [5–9], Fermi surface nesting [10–12], exciton-phonon interactions [13,14], and saddle points near Fermi energy [15,16]. Among these mechanisms, strong electron-phonon interactions can explain some of the key features of the formation of the CDW and seemed most convincing. Conventional CDW transitions can be understood relating to Fermi-surface nesting arising from parallel sections of Fermi-surface sheets. Regarding superconductivity, extensive studies found that the superconducting transition temperature (T_c) is highly dependent on the change of the CDW. A competitive relationship between the CDW and superconductivity has been generally observed [17]. However, the study of phonon dispersion in 2*H*-$NbSe_2$ demonstrated that the CDW transition barely contributes to superconductivity [18]. The angle-resolved photoemission spectroscopy studies indicated that the presence of the CDW order can even boost superconductivity [19]. Thus, although a tremendous amount of research has been carried out, the relationship between superconductivity and the CDW order remains an ongoing puzzle.

For 2*H*-type TMDs, the CDW order can be tuned by metal doping or reducing the dimensionality, yielding the emergence of superconductivity or a pronounced enhancement in superconductivity [20–22]. Besides, pressure has been recognized as a clean and effective tool for modulation of superconductivity and the CDW order in 2*H*-TMDs. In the past few decades, extensive effort has been devoted to explore the pressure effect on the CDW and superconducting states in 2*H*-$NbSe_2$ [3,18,23]; little attention has been paid to 2*H*-TaS_2 with similar crystal and electronic structure to 2*H*-$NbSe_2$. This is due to the relatively low T_c (0.8 K) [4]. Moreover, 2*H*-TaS_2 has only a single transition from a conventional metallic phase to the CDW phase located at 76 K. Recently, Freitas *et al.* [24] found that superconductivity can be significantly enhanced with the suppression of the CDW order. This behavior is different to that in $NbSe_2$. Thus, the high-pressure behavior of TaS_2 is also very important in understanding the physical properties of TMDs. Interestingly, the latest studies [25] reported that the critical pressure, a complete collapse of the CDW, is quite different to that of Freitas's study. Identifying the pressure of the full suppression of CDW order is highly needed. Addressing the interplay between superconductivity and the CDW of TaS_2 is beneficial to understand the origin work of superconductivity in TaS_2 at high pressures.

*xjchen@hpstar.ac.cn

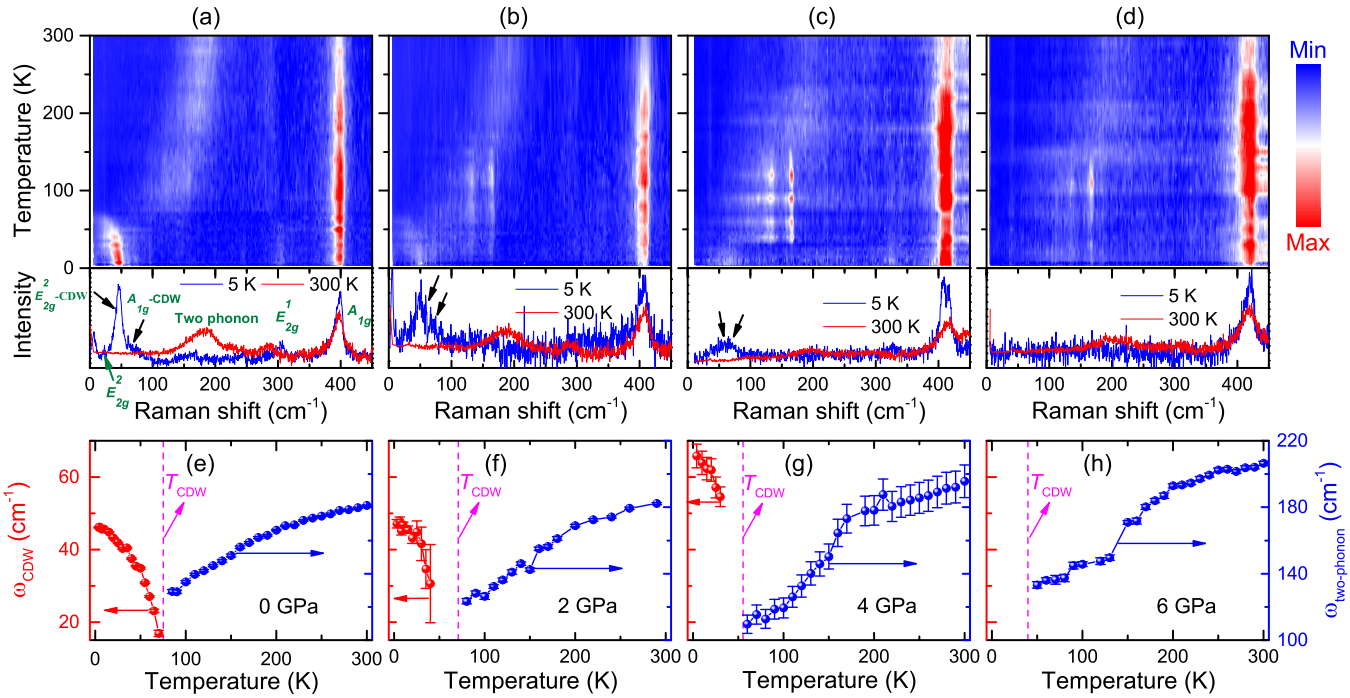

FIG. 1. Raman spectra of 2H-TaS_2 at high pressures and low temperatures. Temperature maps of Raman scattering intensity and the fitted frequencies of CDW and two-phonon modes of TaS_2 at ambient pressure (a), (e), 2 GPa (b), (f), 4 GPa (c), (g), and 6 GPa (d), (h), respectively. Spectra at 5 K and 300 K of each pressure are displayed for clarity. All spectra are subtracted from a constant background, which is independent on temperature. The T_{CDW} of the E^2_{2g}-CDW mode at each pressure is indicated by a vertical dashed line.

In this paper, we report how pressure can efficiently tune both the CDW and superconductivity in TaS_2 though the measurements of Raman spectra, electrical resistivity, and Hall coefficient measurements at high pressures and low pressures. We find that the CDW order shows a gradual reduction with increasing pressure and is fully suppressed above 7.3 GPa, while the value of T_c shows a sharp increase. The relationship between the CDW order and superconductivity is established by the application of pressure. The CDW-superconductivity phase diagram of TaS_2 as a function of pressure is mapped out. The decrease in T_c with pressure is explained above 11.5 GPa. Such studies are found to be critical in understanding the behavior of other TMD materials.

High-quality single crystals of 2*H*-TaS_2 were synthesized at HQ Graphene. For the Raman experiments, all the samples were dissociated to get the fresh surfaces before the measurements. The pressure was obtained by using a diamond anvil cell with anvils in 300 μm culet. The sample was surrounded in the pressure-transmitting medium of neon to ensure hydrostatic pressure conditions in a sample chamber. The Raman scattering spectra were obtained by using a 488-nm sapphire laser beam with the power less than 0.3 mW. The beam was focused on the samples by a $\times 10$ objective. The back scattering light was split by an 1800 lines/mm grating. The low-temperature conditions were obtained by using an *in situ* pressurized superfluid helium cryostat. Additionally, the pressure can be monitored at each temperature interested. High-pressure electrical transport and Hall coefficient measurements were performed by means of the standard four-probe method in Quantum Design's Physical Property Measurement System. The pressure was applied in a nonmagnetic diamond anvil cell [26]. The diamonds were 300 μm in diameter. c-BN was used as the insulating layer. TaS_2 single crystal was cut with the dimensions of 75 μm $*$ 75 μm $*$ 10 μm. Four Pt wires were adhered to the sample using silver epoxy and Daphne oil 7373 was employed as a pressure-transmitting medium. Pressure was determined from the shift of the ruby fluorescence line [27].

I. EVOLUTION OF THE CHARGE DENSITY WAVE WITH PRESSURE

It has been reported that both the high order phonon fluctuations and strong electron-phonon interaction may play important roles in forming the CDW state in this system [28,29]. Raman scattering is recognized as a direct method to reflect the change of the phonon modes. We carried out high-pressure Raman spectra measurements of TaS_2 at different temperatures (Fig. 1) to understand the evolution of the CDW state with pressure. The irreducible representations for 2*H*-TaS_2 are $\Gamma = A_{1g} + E_{1g} + 2E_{2g}$ [30,31]. Here, the E_{1g} mode cannot be observed from both previous reports [32,33] and our measurements because of the near-zero component of the light polarization along the *c* axis. Besides, there is an unusually strong two-phonon (second-order) Raman scattering observed in Raman spectra. This mode is seen in transition metals such as Ta and in transition-metal compounds such as TaC, TiN, and $NbSe_2$, etc.

Figure 1(a) (lower panel) represents the Raman spectra of TaS_2 at 5 K and 300 K. The temperature map of Raman-scattering spectra of TaS_2 at ambient pressure is shown in the upper panel of Fig. 1(a). To analyze the vibrational modes,

we normalized all the spectral intensities by the statistical factor N for the Stokes side by $I(\omega) = I_0(\omega)/[N(\omega, T) + 1]$, where $N(\omega, T)$ is the Bose-Einstein distribution function evaluated at mode energy ω and temperature T, and $I_0(\omega)$ is the observed intensity. As temperature decreased, we found that the two-phonon mode shifts to low frequency and disappears at 75 K [the lock-in temperature of CDW($T_{\rm CDW}$)], while two new peaks appear at around 48 cm^{-1} (E^2_{2g} mode) and 75 cm^{-1} (A_{1g} mode), reminiscent of the Raman active amplitude excitations of the CDW order. Our recent work [32] discovered that the intensity of the A_{1g}-CDW mode is very weak and thus cannot be distinguished for the 488-nm excited spectra. We mainly analyzed the evolution of E^2_{2g}-CDW mode with pressure and temperature. Below $T_{\rm CDW}$, the newly born CDW modes get intensities with decreasing temperature [see Fig. 1(e)]. These findings at ambient pressure are consistent with the previous reports [32,33].

For studying the evolution of the CDW state with pressure, we performed Raman-scattering measurements at high pressures and low temperatures. The Raman spectral maps at different pressures and temperatures are shown in Figs. 1(b)–1(d); we removed the background from the raw data and normalized the data for the clarity. With applied pressure, the CDW mode exhibits blueshift, and the intensity of the CDW mode becomes weak gradually. When pressure is increased to around 6.0 GPa, the CDW mode can hardly be detected, suggesting that CDW order has a strong suppression by the application of pressure. Additionally, the two-phonon mode shows a loss of intensity; the change of the phonon modes may result from the disappearance of the CDW state. A theory presented by Klein [34] indicates that the phonon anomalies in the materials can make important contributions to the two-phonon amplitude. Thus the phonon anomalies result from phonon-assisted scattering of d electrons close to the Fermi level. To precisely analyze the evolution of the CDW mode, Lorentzian function is used to fit the vibrational modes with pressure. The pressure dependencies of the E^2_{2g} CDW and two-phonon modes are plotted out in Figs. 1(e)–1(h). It is worth noting that the temperature dependencies of the CDW and two-phonon modes at high pressures show almost similar behavior to that at ambient pressure. At 2.0 GPa, the two-phonon mode loses its intensity with decreasing temperature and disappears at ∼70 K. Meanwhile, the CDW modes emerge and increase as temperature is decreased. It is clear that $T_{\rm CDW}$ drops gradually with increasing pressure. At 4.0 GPa, $T_{\rm CDW}$ goes down to 56 K. Upon further compression to 6.0 GPa, the two-phonon mode vanishes at about 40 K, accompanied by prodigiously suppressing the CDW modes. The results demonstrated that the CDW order is fully suppressed, or $T_{\rm CDW}$ goes below 5 K at 6.0 GPa. The critical pressure at which the CDW collapse is different from the previous study [24], but there is little difference between our study results and Grasset *et al.*'s report [25]. Interestingly, similar behavior was observed in other TMDs and rare-earth tritellurides [2,18,35], which has been speculated to result from the competition of the superconducting state, because the same electrons are participating in both transitions.

To investigate how pressure affects superconductivity and the relationship between the CDW and superconductivity, we measured the temperature dependence of the electrical transport properties for 2H-TaS_2 up to 47.0 GPa. The evolution of the resistivity with pressure and pressure up to 11.4 GPa are displayed in Fig. 2. There is a conspicuous anomaly in electrical resistivity marked by an arrow, which is clearly associated with an incommensurate CDW [4]. As pressure is increased, $T_{\rm CDW}$ identified from the maximum of $-d_\rho(T)/dT$ drops gradually to low temperature. Above 7.3 GPa, the CDW feature in resistivity was completely suppressed, which is in accord with the results of Raman spectroscopy. The resistivity behaves linearly with temperature and shows a metallic character above $T_{\rm CDW}$. The residual resistivity, or the resistivity in the normal state, steadily decreases with the increase of pressure. Besides the CDW transition, TaS_2 also shows superconductivity at low temperature. To demonstrate superconductivity with more clarity, the inset of Fig. 2 exhibits the temperature dependence of the resistivity below 11.4 GPa at low temperatures. As pressure is increased, T_c shows a continuous increase.

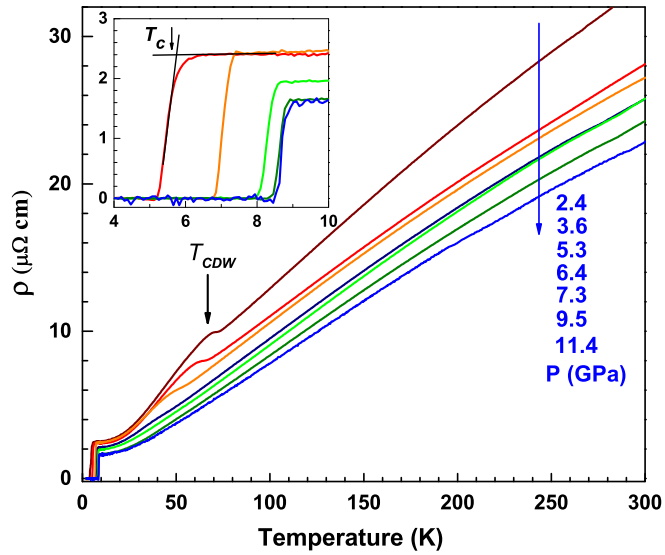

FIG. 2. Electrical resistivity of TaS_2 as a function of temperature at pressures up to 11.4 GPa, $T_{\rm CDW}$ is marked by an arrow. The inset shows superconducting transition within an enlarged region at low temperature and the criterion for determining T_c.

It has been established [32] that the Hall coefficient (R_H) is a very important parameter to investigate the CDW transition. We performed Hall resistivity measurements at 10 K and 300 K up to 47.0 GPa. Motivated by the linear field dependence of resistivity, a one-band Drude approximation was adopted to yield an estimated R_H. The temperature dependence of R_H at ambient pressure is shown in the inset of Fig. 3. It can be seen that R_H is almost independent of temperature at the beginning, and then starts to decrease sharply and changes its sign at a certain temperature 78 K. It has been reported [36] that the R_H in these compounds, which have the CDW transition, is positive above $T_{\rm CDW}$, and then drops quickly and changes its sign below $T_{\rm CDW}$. For the compound without the CDW transition, the R_H is positive over the whole temperature region. Thus, the change of R_H provides another method to determine $T_{\rm CDW}$. The R_H at 10 K and 300 K as a function of pressure are presented in Fig. 3. We found that the R_H at 10 K is negative and the R_H at 300 K is positive at

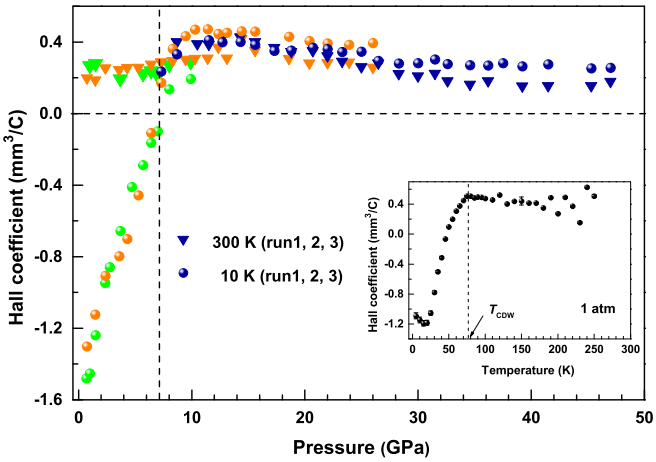

FIG. 3. The inverted triangles and solid circles denote the R_H values of TaS_2 at 300 K and 10 K, respectively. The vertical dashed line indicates the CDW transition. Inset: temperature dependence of R_H values for TaS_2 at ambient pressure.

ambient pressure. With the increase of pressure, R_H at 10 K increases remarkably, while there is almost no change in R_H at 300 K. At the pressure of 7.3 GPa, R_H value at 10 K displays a sign change from negative to positive and is almost equal to that of 300 K, providing more supportive evidence for the collapse of the CDW. As pressure is increased up to 47.0 GPa, it is worth noting that R_H at 10 K and 300 K are both positive, and there is a little difference between the two values.

II. HIGH-PRESSURE PHASE DIAGRAM

Upon heavy compression, the maximum value of T_c (9.3 K) is obtained at 11.5 GPa displayed in Fig. 4, and is nearly eight times the initial value at ambient pressure. After that, T_c decreases consecutively with pressure to the highest pressure studied in the present studies. Simultaneously, the residual resistivity is increased with pressure. This behavior is different to those below 11.5 GPa. What is noteworthy is that the lowest residual resistivity ρ_0 at the pressure of 11.5 GPa responds to the maximum T_c. Now we can analyze the evolution of the electrical resistivity by using the standard resistivity fit, $\rho(T) \simeq \rho_0 + AT^n$, where ρ_0 is the residual resistivity and the prefactor A is related to the pairing interaction strength. The black lines in Fig. 4 are the fitting results. Furthermore, we measured the temperature dependence of the resistivity at different magnetic fields. The results at the pressure of 20.7 GPa are summarized in the inset of Fig. 4. It can be seen that the temperature-dependent resistivity curves gradually shift toward low temperatures with increasing magnetic fields. It seems likely that superconductivity is completely suppressed at 2.5 Tesla, evidencing the superconducting transition in nature.

We have repeated high-pressure measurements on TaS_2 for several independent runs using different samples. The results are highly reproducible. As shown in Fig. 5, we summarized T_{CDW} and T_c as a function of pressure from Raman scattering and resistivity measurements, including some points from previous reports [24,25,37]. As can be seen, T_c of TaS_2 is

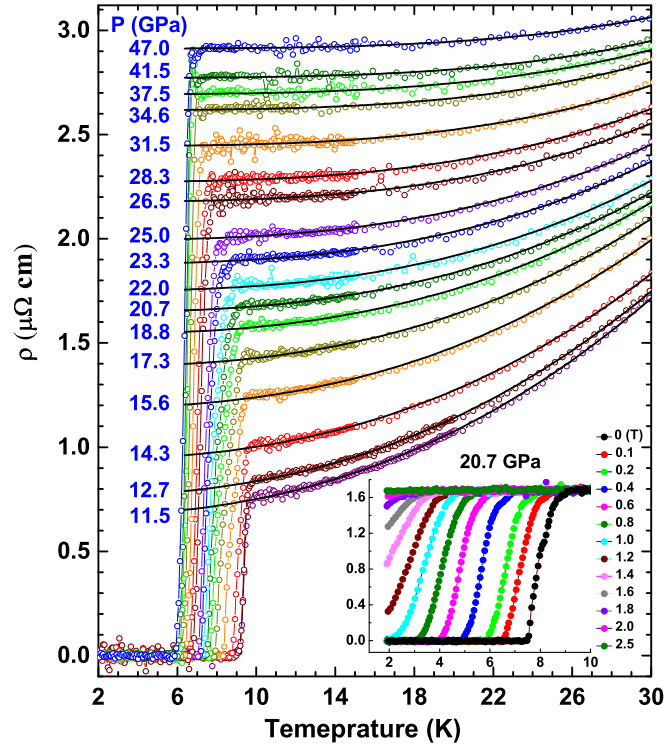

FIG. 4. Temperature dependence of the resistivity of TaS_2 upon further compression to 47 GPa. Raw data were signed with open circles. The black lines are fits to a standard resistivity formula: $\rho(T) \simeq \rho_0 + AT^n$. The inset shows the temperature-dependent resistivity at pressure of 20.7 GPa with the applied magnetic fields.

very low at the beginning, accompanied by the CDW state. A gap opens over part of the Fermi surface in the direction of the q vectors of the CDW, which reduces the average density of states at the Fermi surface and is unfavorable to superconductivity [38]. As the pressure is increased, T_{CDW} drops near

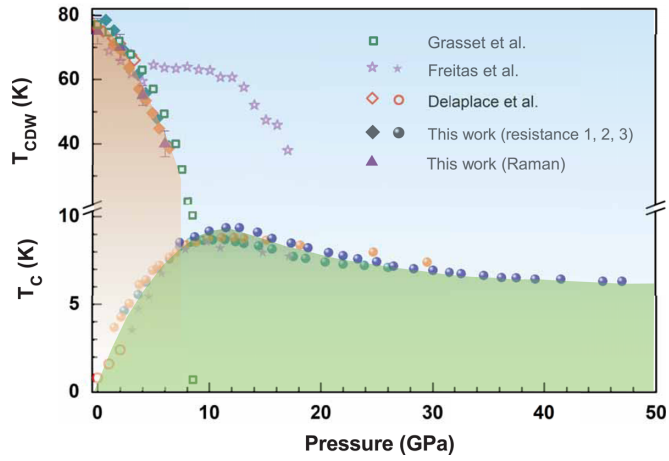

FIG. 5. The phase diagram of 2*H*-TaS_2. Solid rhombuses represent T_{CDW} from the electrical resistivity measurements and the solid circles correspond to T_c; the three independent runs were marked by different colors. Triangles denote T_{CDW} from Raman-scattering measurements. The experimental data points from the work of Refs. [24,25,42] were taken for comparison.

linearly with a coefficient $dT_{CDW}/dP = 7.01 \pm 0.2$ K/GPa and the CDW order is completely suppressed at pressure of around 7.0 GPa. Meanwhile, the value of T_c has an obvious increase. Below 7.0 GPa, there is a coexisting phase of the CDW and superconductivity. With further increasing pressure, T_c has a continuous increase and reaches a maximum of 9.3 K at 11.5 GPa. At higher pressures, $11.5 < P < 47.0$ GPa, T_c has a moderate decrease but still stays above 6.3 K.

The effects of pressure on the CDW and superconductivity has been studied in other similar TMDs such as 2*H*-$NbSe_2$. For this material, the CDW is dramatically suppressed by the application of pressure, while T_c is insensitive to the CDW transition; it was explained that the rapid destruction of CDW is related to the zero mode vibrations—or quantum fluctuations—of the lattice renormalized by the anharmonic part of the lattice potential [18]. Unlike $NbSe_2$, it is found that the CDW for the studied material is suppressed gradually with the application of pressure, while T_c exhibits a significant increase from 1 K at ambient pressure to 8 K at 7.0 GPa. With increasing applied pressure, T_c of TaS_2 continues to increase after the CDW collapses and reaches the maximum at 11.5 GPa, indicating that it is not a simple competition between the CDW and superconductivity. It is noteworthy to mention that the behavior of TaS_2 under pressure is also different from quasi-one-dimensional systems. For the quasi-one-dimensional materials, a superconducting phase sets in after a CDW state has been suppressed [17], or at the critical pressure where the CDW disappears, T_c reaches its maximum value [39,40]. After the disappearance of the CDW, it is possible that the vicinity of a quantum critical point near the collapse of the CDW, and the fluctuations that accompany it, are responsible for the enhancement of T_c.

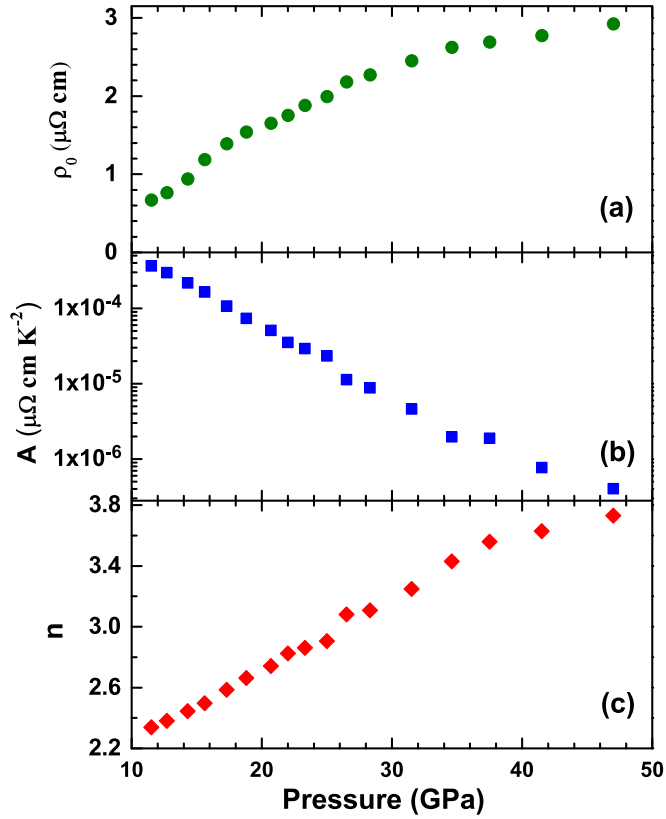

FIG. 6. Fitting parameters from the temperature-dependent resistivity in normal state of TaS_2 at various pressures. (a) Pressure dependence of the residual resistivity ρ_0. (b) Plot of the prefactor A as a function of pressure. (c) The pressure-dependent resistivity exponent n.

III. UNDERSTANDING OF SUPERCONDUCTIVITY UPON COMPRESSION

The presence of the CDW state provides the key understanding for the coexisting region of the CDW order and superconductivity. Above 11.5 GPa, the standard resistivity formula was employed to fit the resistivity in the normal state (see Fig. 4). The resistivity exponent n, the residual resistivity ρ_0, and the prefactor A were obtained through a fitting procedure over the low-temperature region of up to 30 K (shown in Fig. 6). For the pressure range from 11.5–47.0 GPa, the resistivity exponent n was found to increase from 2.3 to 3.7. Those values are different from the expected value of $n = 2$ or $n = 5$ for electron-electron or electron-phonon scattering [41,42], respectively. Similarly, there are some rare cases in $TiSe_2$ ($n \simeq 2.6$) [2] and $NbPt_3$ ($n = 3$) [43]. Those n values are commonly attributed to a phonon-assisted *s-d* interband scattering. A report from Wilson [44] explains how scattering from a low-mass band into a high-density band can yield higher power-law temperature-dependent resistivity. The prefactor A exhibits a continuous decrease in the pressure range. Empirically, there exists a relationship between A and T_c, the stronger the pairing interaction strength is, the higher T_c is [42]. The gradual decrease of T_c above 11.5 GPa is considered to obey this relationship. Meanwhile, the residual resistivity ρ_0, related to impurity scattering, shows a steady increase upon compression. A strong correlation between T_c and ρ_0 was proposed in a previous study, the impurity scattering is not in favor of T_c enhancement [45]. The decline of T_c after passing of a maximum is due to the decrease of the interaction strength and the increase of the impurity scattering.

In summary, we have carried out measurements of electrical resistivity, Hall coefficient, and the Raman spectra on TaS_2 at high pressures and low temperatures. The CDW order was observed to disappear at a pressure of 7.0 GPa, which is accompanied by the sign change of the Hall coefficient. A strong correlation among the critical temperature, residual resistivity, and prefactor A is uncovered by fitting resistivity in the normal state; both the stronger impurity scattering and weaker phonon-assisted *s-d* interband scattering with the increase of pressure account for the gradual decrease in T_c above 11.5 GPa. Our results revealed the distinct pressure-tunable characteristics of TaS_2 and addressed the relationship between the CDW and superconductivity.

ACKNOWLEDGMENTS

This project was supported by the Doctoral Fund of Henan University of Technology under Grant No. 2018BS004 and the Fundamental Research Funds for the Henan Provincial Colleges and University of Technology under Grant No. 2018QNJH29, and the Science and Technology Foundation

of Henan province education department under Grant No. 20A140011. The electrical transport measurements were supported by the DOE under Grant No. DE-FG02-02ER45955. A.G.G. acknowledges support of Grant No. RScF 16-12-10464. For preparation of high-pressure cells, the facilities of the Center for Collective Use Accelerator Center for Neutron Research of the Structure of Substance and Nuclear Medicine of the INR RAS were used.

[1] B. Sipos, A. F. Kusmartseva, A. Akrap, H. Berger, L. Forró, and E. Tutiš, Nat. Mater. **7**, 960 (2008).
[2] A. F. Kusmartseva, B. Sipos, H. Berger, L. Forró, and E. Tutiš, Phys. Rev. Lett. **103**, 236401 (2009).
[3] C. Berthier, P. Molinié, and D. Jérome, Solid State Commun. **18**, 1393 (1976).
[4] S. Nagata, T. Aochi, T. Abe, S. Ebisu, T. Hagino, Y. Seki, and K. Tsutsumi, J. Phys. Chem. Solids **53**, 1259 (1992).
[5] F. Weber, S. Rosenkranz, J. P. Castellan, R. Osborn, R. Hott, R. Heid, K. P. Bohnen, T. Egami, A. H. Said, and D. Reznik, Phys. Rev. Lett. **107**, 107403 (2011).
[6] T. Valla, A. V. Fedorov, P. D. Johnson, P. A. Glans, C. McGuinness, K. E. Smith, E. Y. Andrei, and H. Berger, Phys. Rev. Lett. **92**, 086401 (2004).
[7] L. P. Gor'kov, Phys. Rev. B **85**, 165142 (2012).
[8] X. Zhu, J. Guo, J. Zhang, and E. W. Plummer, Adv. Phys.: X **2**, 622 (2017).
[9] K. Wijayaratne, J. Zhao, C. Malliakas, D. Y. Chung, M. G. Kanatzidis, and U. Chatterjee, J. Mater. Chem. C **5**, 11310 (2017).
[10] S. V. Borisenko, A. A. Kordyuk, A. N. Yaresko, V. B. Zabolotnyy, D. S. Inosov, R. Schuster, B. Büchner, R. Weber, R. Follath, L. Patthey, and H. Berger, Phys. Rev. Lett. **100**, 196402 (2008).
[11] S. V. Borisenko, A. A. Kordyuk, V. B. Zabolotnyy, D. S. Inosov, D. Evtushinsky, B. Büchner, A. N. Yaresko, A. Varykhalov, R. Follath, W. Eberhardt, L. Patthey, and H. Berger, Phys. Rev. Lett. **102**, 166402 (2009).
[12] M. D. Johannes, I. I. Mazin, and C. A. Howells, Phys. Rev. B **73**, 205102 (2006).
[13] J. van Wezel, P. Nahai-Williamson, and S. S. Saxena, Phys. Rev. B **83**, 024502 (2011).
[14] C. Monney, C. Battaglia, H. Cercellier, P. Aebi, and H. Beck, Phys. Rev. Lett. **106**, 106404 (2011).
[15] T. M. Rice and G. K. Scott, Phys. Rev. Lett. **35**, 120 (1975).
[16] K. Rossnagel, J. Phys.: Condens. Matter **23**, 213001 (2011).
[17] R. Yomo, K. Yamaya, M. Abliz, M. Hedo, and Y. Uwatoko, Phys. Rev. B **71**, 132508 (2005).
[18] M. Leroux, I. Errea, M. Le Tacon, S.-M. Souliou, G. Garbarino, L. Cario, A. Bosak, F. Mauri, M. Calandra, and P. Rodière, Phys. Rev. B **92**, 140303(R) (2015).
[19] T. Kiss, T. Yokoya, A. Chainani, S. Shin, T. Hanaguri, M. Nohara, and H. Takagi, Nat. Phys. **3**, 720 (2007).
[20] K. E. Wagner, E. Morosan, Y. S. Hor, J. Tao, Y. Zhu, T. Sanders, T. M. McQueen, H. W. Zandbergen, A. J. Williams, D. V. West, and R. J. Cava, Phys. Rev. B **78**, 104520 (2008).
[21] E. Navarro-Moratalla, J. Island, S. Mañas-Valero, E. Pinilla-Cienfuegos, A. Castellanos-Gomez, J. Quereda, G. Rubio-Bollinger, L. Chirolli, J. Silva-Guillén, N. Agraít, G. Steele, F. Guinea, H. van der Zant, and E. Coronado, Nat. Commun. **7**, 11043 (2016).
[22] Y. Yang, S. Fang, V. Fatemi, J. Ruhman, E. Navarro-Moratalla, K. Watanabe, T. Taniguchi, E. Kaxiras, and P. Jarillo-Herrero, Phys. Rev. B **98**, 035203 (2018).
[23] R. Grasset, T. Cea, Y. Gallais, M. Cazayous, A. Sacuto, L. Cario, L. Benfatto, and M.-A. Méasson, Phys. Rev. B **97**, 094502 (2018).
[24] D. C. Freitas, P. Rodière, M. R. Osorio, E. Navarro-Moratalla, N. M. Nemes, V. G. Tissen, L. Cario, E. Coronado, M. García-Hernández, S. Vieira, M. Núñez-Regueiro, and H. Suderow, Phys. Rev. B **93**, 184512 (2016).
[25] R. Grasset, Y. Gallais, A. Sacuto, M. Cazayous, S. Mañas-Valero, E. Coronado, and M. A. Méasson, Phys. Rev. Lett. **122**, 127001 (2019).
[26] A. G. Gavriliuk, A. A. Mironovich, and V. V. Struzhkin, Rev. Sci. Instrum. **80**, 043906 (2009).
[27] H. K. Mao, P. M. Bell, J. W. Shaner, and D. J. Stembey, J. Appl. Phys. **49**, 3276 (1978).
[28] J. E. Inglesfield, J. Phys. C: Solid State Phys. **13**, 17 (1980).
[29] C. M. Varma and A. L. Simons, Phys. Rev. Lett. **51**, 138 (1983).
[30] S. Sugai, K. Murase, S. Uchida, and S. Tanaka, Solid State Commun. **40**, 399 (1981).
[31] M. Hangyo, S. I. Nakashima, and A. Mitsuishi, Ferroelectrics **52**, 151 (1983).
[32] K. Zhang, Z. Cao, and X. J. Chen, Appl. Phys. Lett. **114**, 141901 (2019).
[33] J. Joshi, H. M. Hill, S. Chowdhury, C. D. Malliakas, F. Tavazza, U. Chatterjee, A. R. Hight Walker, and P. M. Vora, Phys. Rev. B **99**, 245144 (2019).
[34] M. V. Klein, Phys. Rev. B **24**, 4208 (1981).
[35] D. A. Zocco, J. J. Hamlin, K. Grube, J.-H. Chu, H.-H. Kuo, I. R. Fisher, and M. P. Maple, Phys. Rev. B **91**, 205114 (2015).
[36] M. Naito and S. Tanaka, J. Phys. Soc. Jpn. **51**, 219 (1982).
[37] R. Delaplace, P. Molinie, and D. Jerome, J. Phys. Lett. **37**, 1 (1994).
[38] For a general discussion, see *Crystal Chemistry and Properties of Materials with Quasi-One-Dimensional Structures*, edited by J. Rouxel (D. Reidel Publishing, Dordrecht, 1986).
[39] M. Regueiro, J. Mignot, and D. Castello, Europhys. Lett. **18**, 53 (1992).
[40] M. Monteverde, J. Lorenzana, P. Monceau, and M. Núñez-Regueiro, Phys. Rev. B **88**, 180504(R) (2013).
[41] D. Forsythe, S. R. Julian, C. Bergemann, E. Pugh, M. J. Steiner, P. L. Alireza, G. J. McMullan, F. Nakamura, R. K. W. Haselwimmer, I. R. Walker, S. S. Saxena, G. G. Lonzarich, A. P. Mackenzie, Z. Q. Mao, and Y. Maeno, Phys. Rev. Lett. **89**, 166402 (2002).
[42] M. Núñez-Regueiro, G. Garbarino and M. D. Núñez-Regueiro, J. Phys.: Conf. Ser. **400**, 022085 (2012).
[43] R. Caton and R. Viswanathan, Phys. Rev. B **25**, 179 (1982).
[44] A. H. Wilson, Proc. R. Soc. A **167**, 580 (1938).
[45] I. I. Mazin, O. K. Andersen, O. Jepsen, O. V. Dolgov, J. Kortus, A. A. Golubov, A. B. Kuz'menko, and D. van der Marel, Phys. Rev. Lett. **89**, 107002 (2002).